LITERATURE CITED

Bier, M., "A New Principle of Preparative Electrophoresis," *Science*, **125**, 1084 (1957).

Caldwell, K. D., L. F. Kesner, M. N. Meyers, and J. C. Giddings, "Electrical Field-Flow Fractionation of Proteins," *ibid.*, **176**, 296 (1972).

Giddings, J. C., "A New Separation Concept Based on a Coupling of Concentration and Flow Nonuniformities," *Separation Science*, **1**, No. 1, 123 (1966).

Hannig, K., "Eine Neuentruicklung der Trägerfreien Knotinuirlichen Elektrophorese," *Z. für Physiol. Chemie*, 338, 211 (1964).

———., "The Application of Free-Flow Electrophoresis to the Separation of Macromolecules and Particles of Biological Importance," in *Modern Separation Methods of Macromolecules and Particles*, Theo Gerritsen, ed., Wiley-Interscience, New York (1969).

Kirkwood, J. G., "A Suggestion for a New Method of Fractionation of Proteins by Electrophoresis-Convection," *J. Chem. Phys.*, **9**, 878 (1941).

Lee, H-L, J. F. G. Reis, J. Dohner, and E. N. Lightfoot, "Single Phase Chromatography: Solute Retardation by Ultrafiltration and Electrophoresis," *AIChE J.*, **20**, No. 4, 776 (1974).

Lowry, O. H., N. J. Rosebrough, and R. J. Randall, "Protein Measurement with the Folin Reagent," *J. Biol. Chem.*, **193**, 265 (1951).

Reis, J. F. G., E. N. Lightfoot, and H-L Lee, "Concentration Profiles in Free-Flow Electrophoresis," *AIChE J.*, **20**, No. 2, 362 (1974).

Reis, J. F. G., A. Shah, and E. N. Lightfoot, "Comparison between Electropolarization Chromatography and Free-Flow Electrophoresis," *ibid.*, to be proposed for publication.

Tiselius, A., "A New Apparatus for Electrophoretic Analysis of Colloidal Mixtures," *Trans. Faraday Soc.*, 33, 524 (1937).

Manuscript received January 19, 1976; revision received and accepted April 20, 1976.

Design of An Ionic Lattice for Optimum Cation Diffusion

ELI RUCKENSTEIN

and

DADY B. DADYBURJOR

Faculty of Engineering and Applied Sciences
State University of New York at Buffalo
Buffalo, NY 14214

Varying the species and/or distance parameters of a lattice changes the activation energy of a particular species diffusing through it, thus allowing transport properties to be optimized. As an example, the activation energy of silver ions in α-silver iodidelike structures was calculated as lattice properties were changed.

SCOPE

The interaction between an ion moving in a lattice and another ion that is part of the lattice consists of coulombic, shell repulsion, induced dipole, and other energy terms. The mobile ion has a preferred path where the total energy, summed for all other ions, is always a minimum. This minimum energy as a function of the coordinate in the direction of motion has peaks and valleys. The difference between these extrema is an activation energy of transport of the ion and hence plays a part in determining the diffusivity and conductivity. Flygare and Huggins (1973) varied the ionic radius of the mobile cations through the α-silver iodidelike lattice and found that the activation energy was a minimum (and hence ion transport was easiest) at an ionic radius close to the value determined experimentally for Ag^+. Hence, the observed high conductivity and diffusivity of silver ions in α-silver iodide were directly related to the minimum in the activation energy for ionic transport.

In this work we suggest the inverse problem, the determination of lattice parameters so as to minimize the activation energy of transport for a given species. This simple turnabout has vast potential applications. For example, it may be possible to design lattices for compounds to be used as solid electrolytes in fuel cells and batteries to minimize activation energies for mobile cations. At the present moment, the investigation and selection of these often complex materials is done on a case-by-case basis. (See, for instance, Hoshino, 1955; Geller and Lind, 1970; Geller, 1972.) A similar technique can also help in the design of an optimum catalyst. Batist et al. (1968) suggested that, at low temperatures, controlled diffusion of oxygen through the bismuth molybdate structure is important in the catalytic oxidation of 1-butene to butadiene. It may be possible to calculate the structure of a lattice that will give rise to the corresponding activation energy for oxygen diffusion and thus improve the selectivity of the catalyst.

As a simple example we consider below the determination of an α-silver lattice to minimize transport of silver cations. This may be of value in the design of solid electrolytes (van Gool, 1974).

CONCLUSIONS AND SIGNIFICANCE

The technique is of value in determining lattice structures that optimize transport of a specified species. In the example considered, the activation energy increased monotonically as lattice parameters were linearly varied from those of α-Ag_2S to those of α-Ag_2Se. These bcc (body centered cubic) monodivalent compounds in general had lower activation energies than those of a fcc (face centered cubic) monodivalent compound (α-Ag_2Te) or a bcc monomonovalent compound (α-AgI). For a hypothetical lattice having the α-AgI structure but an increased charge on the mobile cation, the activation energy passed through extrema as the lattice parameters were varied.

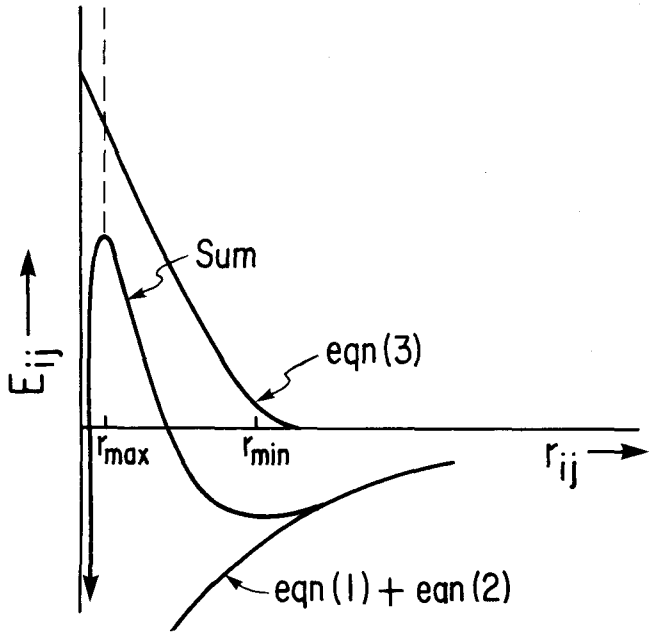

Fig. 1. Interaction energy between a mobile and a lattice ion. The artificial maximum is at r_{max}; the mathematical expression diverges at smaller r_{ij}. The assumed energy profile in that region is also shown (- - -).

CALCULATION OF THE ACTIVATION ENERGY FROM ION-ION INTERACTIONS

An ion that is free to move in a stationary ionic lattice has a total energy of interaction which may be considered as the sum of interaction energies of the mobile ion with each of the other ions. The total interaction energy of the mobile ion is therefore dependent upon its position in the lattice, the lattice parameters, and the properties of the ions. For motion along any of the three direction coordinates of the lattice, the mobile ion will always be positioned with respect to the two other direction coordinates such that its total interaction energy is a minimum. The total interaction energy along this preferred path plotted as a function of the lattice coordinate in the direction of motion is termed the energy path in what follows. The difference between the highest peak and the lowest valley of the energy path for a given mobile ion-lattice system is clearly the minimum additional energy required by the mobile ion to travel through the stationary lattice and hence is termed the activation energy of interaction. In this section we calculate the total interaction energy of the mobile ion and show how the activation energy for the ion-lattice system can, in principle, be obtained.

Consider first the interaction with a single ion. The coulombic energy term $E_{ij,c}$ between a mobile ion of algebraic charge z_ie and an ion of algebraic charge z_je (monopole-monopole interaction) is given by

$$E_{ij,c} = e^2 z_i z_j / r_{ij} \tag{1}$$

where r_{ij} is the interionic distance. Further, each of the ions induces a dipole in the other and interacts with it. This monopole-induced dipole interaction is written (Hirschfelder et al., 1954)

$$E_{ij,d} = -\frac{1}{2}\alpha_j (z_i e)^2 / r_{ij}^4 - \frac{1}{2}\alpha_i (z_j e)^2 / r_{ij}^4 \tag{2}$$

where the α's are the ionic polarizabilities. We ignore the considerably less significant multipole-multipole interaction. The electron shell overlap repulsion energy has been written (Pauling, 1928; Cubiccioti, 1959)

$$E_{ij,s} = c_{+-} b \exp[(r_i + r_j - r_{ij})/\rho] \tag{3a}$$

where c_{+-} is the overlap constant

$$c_{+-} = 1 + \frac{z_i}{N_i} + \frac{z_j}{N_j} \tag{3b}$$

b is the repulsion constant, r_i and r_j are the ionic radii, and ρ is the repulsion parameter. N_i and N_j are the number of electrons in the outermost shell of each of the two ions.

Figure 1 illustrates the sum of Equations (1) through (3) for the interaction between two oppositely charged ions. At medium and large separation distances, the shape of the potential is well represented by the curve. Note particularly the minimum corresponding to the equilibrium position of the cation. At small values of r_{ij}, however, Equation (2) diverges, leading to a maximum and a steep drop to $-\infty$ for the total interaction energy. This has no basis in reality, since we expect the repulsion potential for very small separations to be much greater than given by Equation (3a). The problem can be avoided by postulating a lower limit of r_{ij} for which the equations hold, $r_{ij} > r_{max}$, where r_{max} is the position of the artificial maximum. For values of $r_{ij} \leq r_{max}$, the total interaction energy E_{ij} is set equal to $+\infty$.

A coordinate system for calculating the separation distance r_{ij} of the mobile ion from one of a large number of other ions is given below. Since the lattice is composed of a large number of repeating structures on all sides of the mobile ion, the origin of the coordinate system is taken to be one of the corners of the unit cell containing the mobile ion. The coordinates of the mobile ion are then $(c_1 l, c_2 m, c_3 n)$, where c_1, c_2, c_3 are the lattice parameters and where $0 \leq l, m, n < 1$. Hence the distance between the mobile ion and a corner ion located X, Y, Z unit cells in the l, m, n directions, respectively, is

$$r_{ij} = [c_1^2(X - l)^2 + c_2^2(Y - m)^2 + c_3^2(Z - n)^2]^{1/2} \tag{4a}$$

where X, Y, Z are integers, not necessarily positive. Here

we have taken the lattice directions to be mutually perpendicular; this assumption is not unduly restrictive and can be easily removed. In the more general case, where the j_{-th} ion of the $(X, Y, Z)_{-th}$ unit cell in the lattice is at the position $(c_1 f_{1j}, c_2 f_{2j}, c_3 f_{3j})$, the interionic distance is

$$r_{ij}(X, Y, Z) = [c_1^2(X + f_{1j} - l)^2 + c_2^2(Y + f_{2j} - m)^2 + c_3^2(Z + f_{3j} - n)^2] \quad (4b)$$

From Equations (1) through (3), the interaction energy of a mobile ion situated at the reduced coordinates (l, m, n) inside a lattice containing J ions per unit cell is

$$E(c; l, m, n) = \sum_Z \sum_Y \sum_{X=-\infty}^{\infty} \sum_{j=1}^{J} A\,[r_{ij}(X, Y, Z)]^{-4} + \sum_Z \sum_Y \sum_{X=-\infty}^{\infty} \sum_{j=1}^{J} B \exp[-r_{ij}(X, Y, Z)/\rho] + \sum_Z \sum_Y \sum_{X=-\infty}^{\infty} \sum_{j=1}^{J} C\,[r_{ij}(X, Y, Z)]^{-1} \quad (5)$$

where

$$A = -\frac{1}{2} e^2(z_i^2 \alpha_j + z_j^2 \alpha_i)$$

$$B = c_{+-} b \exp[(r_i + r_j)/\rho]$$

$$C = e^2 z_i z_j$$

and $r_{ij}(X, Y, Z)$ is given by Equation (4b). It should be noted that in Equations (5) the subscript and summation index j refer to any ion other than the test ion, subscript i; the species of j may or may not be the same as that of the mobile ion, i. For a simple cubic lattice

$$J = 1 \quad (6a)$$

$$f_{1,1} = f_{2,1} = f_{3,1} = 0 \quad (6b)$$

$$c_1 = c_2 = c_3 \quad (6c)$$

while for a body centered cubic (bcc) structure

$$J = 2 \quad (6d)$$

$$f_{1,1} = f_{2,1} = f_{3,1} = 0 \quad (6e)$$

$$f_{1,2} = f_{2,2} = f_{3,2} = 0.5 \quad (6f)$$

$$c_1 = c_2 = c_3 \quad (6g)$$

The face centered cubic (fcc) lattice can be treated as a body centered tetragonal so that the values of J and the f's are as in the bcc case and

$$c_1 = c_2 = c_f/\sqrt{2} \quad c_3 = c_f \quad (6h)$$

where c_f is the parameter of the fcc lattice.

For definiteness, we will consider the cation to be moving along the l axis. For each value of l, it will occupy the position of minimum energy; that is, its coordinates $m^*(l)$ and $n^*(l)$ are such that

$$\frac{\partial}{\partial m} E(c; l, m^* n^*) = 0 = \frac{\partial}{\partial n} E(c; l, m^* n^*) \quad (7)$$

with

$$\frac{\partial^2 E}{\partial m^2} \text{ and } \frac{\partial^2 E}{\partial n^2} > 0; \quad \left(\frac{\partial^2 E}{\partial m^2}\right)\left(\frac{\partial^2 E}{\partial n^2}\right) > \left(\frac{\partial^2 E}{\partial m \partial n}\right)^2 \quad (8)$$

However, in defining the positions of minimum energy, problems arise that are similar to the problem illustrated for the interaction with a single ion in Figure 1. Following what was done earlier, we ignore the decreasing interaction energies generated by the form of Equations (1), (2), and (3) at small values of $r_{ij}(X, Y, Z)$ for any j. Further, we set E equal to $+\infty$ for values of l, m, and n corresponding to the artificial maximum for any ion. This effectively excludes the mobile ion from entering spheres centered at the center of the other ions. The excluded zone is treated in greater detail in a later section.

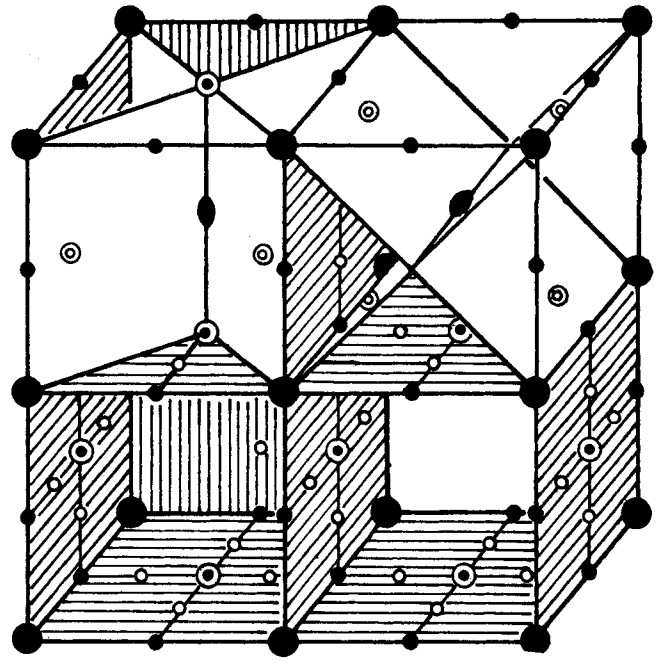

Fig. 2. Model for α-Ag^+ compounds showing the thirty most favorable positions for cations (Strock, 1934).

⊙ and · e type (6/unit cell)
○ h type (12/unit cell)
○○ n type (12/unit cell)
● iodide anion (fixed)

See text for explanation.

By writing $E^*(c; l) \equiv E(c; l, m^*, n^*)$, the activation energy for these values of the lattice parameters $\Delta E(c)$ can be written

$$\Delta E(c) = E^*(c; l_{max}) - E^*(c; l_{min}) \quad (9)$$

where l_{max} and l_{min} both satisfy

$$\frac{\partial}{\partial l} E^*(c; l) = 0 \quad (10)$$

except that

$$\frac{\partial^2}{\partial l^2} E^*(c, l_{max}) < 0 \quad (11a)$$

and

$$\frac{\partial^2}{\partial l^2} E^*(c, l_{min}) > 0 \quad (11b)$$

APPLICATION TO THE α-SILVER COMPOUNDS

Sample calculations are performed on α-silver iodide-like compounds to calculate the activation energy of transport (in this case, of Ag^+ ions) when lattice parameters are changed. The existence of high electrical conductivity and ionic diffusion in these solids has been known for many years. Strock (1934), in a carefully thought out analysis, showed that these properties occur in α-silver iodide because all cations are free to move and all anions are stationary. His model is illustrated in Figure 2. The iodide ions occupy a body cen-

tered cubic (bcc) lattice; that is, there are two anions per unit cell. On the average there will be two Ag^+ ions per unit cell. Each of these would be moving into or out of one of thirty of the largest holes in the unit cell. Six of these holes would be of the e type, at the midpoint of an edge or at the center of a face; twelve would be of the h type, at the midpoint of the line joining the midpoint of an edge to a face passing through the edge; the remaining twelve would be of the n type, on the line joining the midpoints of two edges diagonally opposite each other.

For the case of α-AgI, the subscript i in Equation (5) denotes a test mobile Ag^+ cation, while j denotes the other (mobile) Ag^+ ions in the lattice as well as the stationary I^- anions. The test mobile cation is at $(c_1 l,\ c_1 m,\ c_1 n)$. Clearly, $J = 4$ for this lattice (two cations and two anions). The coordinates of the two stationary anions are

$$f_{1,1} = f_{2,1} = f_{3,1} = 0 \qquad (12a)$$

for the corner ions, and

$$f_{1,2} = f_{2,2} = f_{3,2} = 0.5 \qquad (12b)$$

for the center ions. The positions of the other mobile cations are, by definition, not fixed. However, we ignore the monopole-induced dipole interactions between the test mobile ion and the other Ag^+ ions on the grounds that the cation polarizability is greatly overshadowed by that of the anion. Indeed, the polarizability is related to the cube of the ionic radius (Rice, 1940), and the anionic radius here is much greater than that of the cation. We also ignore the closed shell repulsion between two cations on the grounds that it represents a very close-range interaction. Following Flygare and Huggins (1973), we postulate that the coulomb repulsions due to the presence of other mobile cations are exactly counterbalanced by the coulomb attractions between stationary and mobile ions. By following these arguments, Equation (5) for the special case of the α-AgI lattice can be rewritten as

$$E(c_1; l, m, n) = \sum_Z \sum_Y \sum_{X=-\infty}^{\infty} A\,[r_{i1}^{-4}(X, Y, Z) + r_{i2}^{-4}(X, Y, Z)] + \sum_Z \sum_Y \sum_{X=-\infty}^{\infty} B \left\{ \exp\left[-\frac{r_{i1}(X, Y, Z)}{\rho}\right] + \exp\left[-\frac{r_{i2}(X, Y, Z)}{\rho}\right] \right\} \qquad (13)$$

where

$$A = -\frac{1}{2} e^2 z_i^2 \alpha_j$$

$$B = c_{+-} b \exp[(r_i + r_j)/\rho]$$

$$r_{i1}(X, Y, Z) = c_1[(X - l)^2 + (Y - m)^2 + (Z - n)^2]^{1/2}$$

$$r_{i2}(X, Y, Z) = c_1[(X - l + 0.5)^2 + (Y - m + 0.5)^2 + (Z - n + 0.5)^2]^{1/2}$$

α_j and r_j are now the polarizability, and ionic radius of the stationary anion. Note that we have replaced $\mathbf{c}$ by c_1 in the left-hand side of Equation (13) owing to the cubic nature of the anionic lattice. The cation polarizability α_i has been set equal to zero.

Recall that we are designing a crystal lattice to optimize transport of Ag^+ ions by minimizing the activation energy as discussed in the previous section. In order to have a basis for comparison, and for computational consistency, we have considered only silver compounds with the α-silver iodide structure. This puts a serious constraint on the variables, since the only compounds that qualify (Rahlfs, 1936) are the sulfide Ag_2S and the selenide Ag_2Se. Since they are of the form Ag_2X, the unit cells contain on the average four, and not two, of the thirty holes filled with cations. However, Equation (13) can still be used for these compounds. The telluride also has the α form, but the anionic lattice is face centered cubic (fcc). As shown before, this requires a modification to Equation (13) in that

$$r_{i1}(X, Y, Z) = (c_f/\sqrt{2})[(X - l)^2 + (Y - m)^2 + 2(Z - n)^2]^{1/2} \qquad (14a)$$

and

$$r_{i2}(X, Y, Z) = (c_f/\sqrt{2})[(X - l + 0.5)^2 + (Y - m + 0.5)^2 + 2(Z - n + 0.5)^2]^{1/2} \qquad (14b)$$

where c_f is the fcc lattice parameter. For the compounds of interest, the anionic parameters of Equations (13) and (14) are listed in Table 1. The repulsion constant b is set equal to 1×10^{-12} erg, and the parameter ρ is given an average value of 0.333Å for the Ag^+ cation. The cationic charge integer z_i is clearly +1. The ionic radii were taken from Shannon and Prewitt (1969). To ensure consistency, all values were for a coordination number of 6. The polarizabilities were calculated from values of the gram-atomic refractivity tabulated by Rich (1965). The cell lengths were taken from those collected by Donnay (1963).

Table 1. Anionic Parameters for α-Silver Compounds

	r_j Å	c_1 Å	α_j Å^3	z_j	c_{+-}
Ag_2S	1.84	4.89	3.06	−2	$\frac{29}{36}$
Ag_2Se	1.98	4.99	4.29	−2	$\frac{29}{36}$
AgI	2.20	5.044	5.58	−1	$\frac{67}{72}$
Ag_2Te	2.21	6.585	5.71	−2	$\frac{29}{36}$

Following the suggestion of Strock (1934), we assumed that the sulfide and the selenide could be mixed in all proportions. The properties of the mixture were taken to be linearly varying from those of one pure compound to those of the other. It is reasonable to assume this, since the anionic lattices have the same form and the ionic valences are equal. However, for the iodide, the anionic valence is not that of the previous two compounds; similarly, the structure of the telluride is not bcc. Hence there is no basis for assuming that mixtures of any of these with either of the previous compounds would even exist in all proportions, much less have a definable structure. The iodide and the telluride were not considered in the mixing process.

From interpolation between the sulfide and selenide properties in Table 1, the properties of the hypothetical mixture were written in terms of the lattice parameter c_1:

$$r_j = 1.4\, c_1 - 5.006$$

$$\alpha_j = 12.3\, c_1 - 57.087 \qquad (15)$$

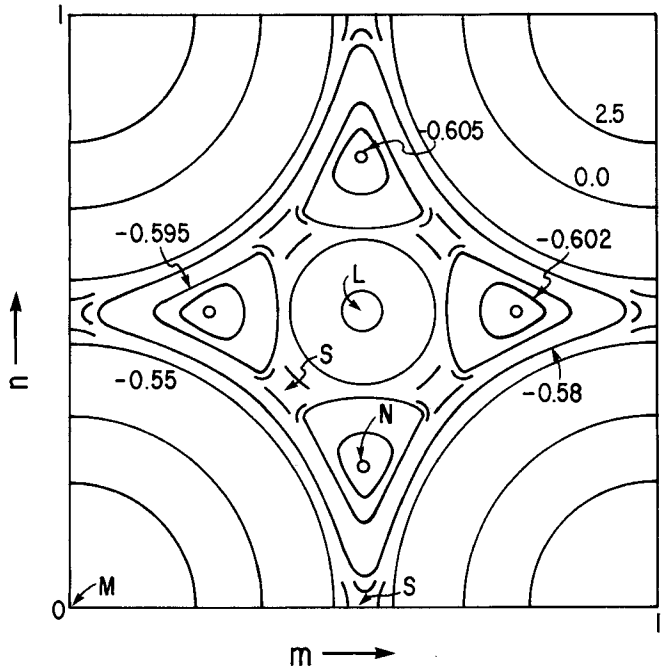

Fig. 3. Energy profile for Ag^+ in α-AgI at $l = 0$. See text for parameters. Numbers indicate value of interaction energy along equipotential lines in 10^{-11} erg. L—position of local maximum; M—position of (fixed) anion; N—position of minimum; S—saddle point.

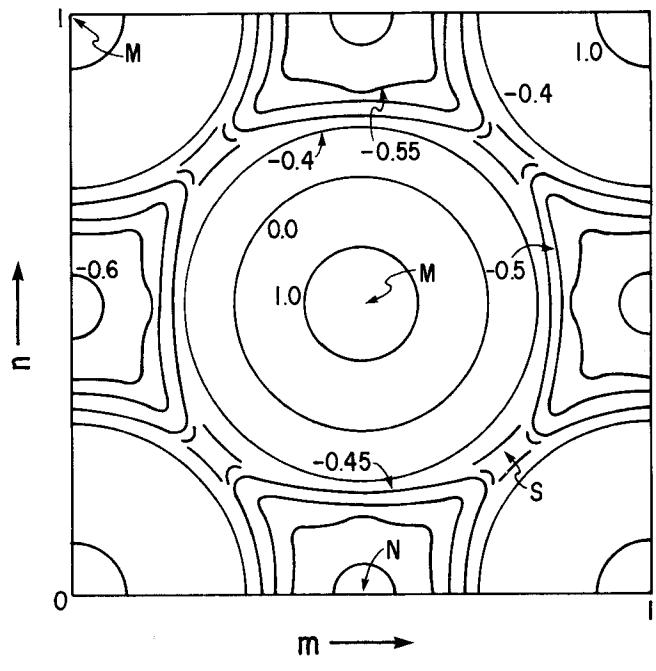

Fig. 4. Energy profile for Ag^+ in α-AgI at $l = 0.25$. See Figure 3 for explanation.

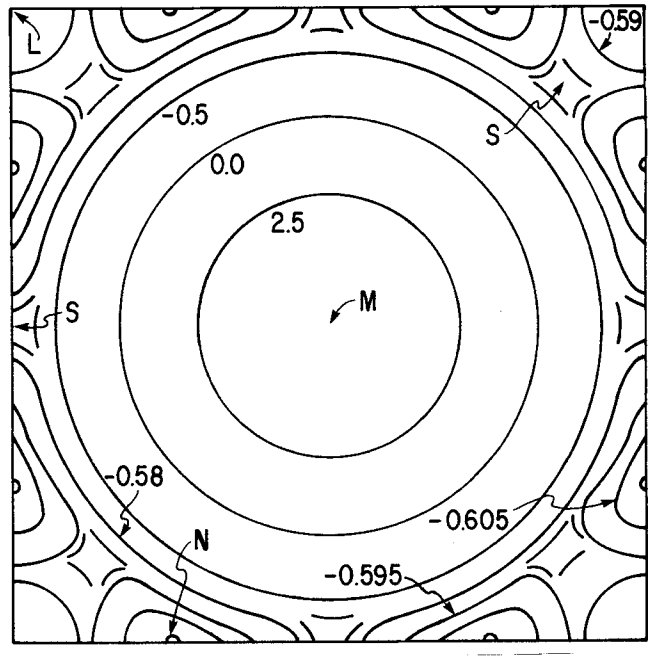

Fig. 5. Energy profile of Ag^+ in α-AgI at $l = 0.5$. See Figure 3 for explanation.

The values of $\Delta E(c_1)$ for various values of c_1 are obtained in a following section.

ENERGY PROFILES

Figures 3, 4, and 5 show equipotential lines at $l = 0$, 0.25, and 0.5, respectively, as felt by a cation moving along a unit cell of the bcc anionic lattice of α-AgI. These energy profiles were computed by substituting the parameters suggested by Flygare and Huggins (1973), namely, $z_i = 1$, $z_j = -1$, $c_{+-} = 1$, $\alpha_j = 6.43\text{Å}^3$, $c_1 = 5.034\text{Å}$, $r_i = 1.75\text{Å}$, $r_j = 0.8\text{Å}$, $\rho = 0.333\text{Å}$, in Equations (13). The summation was carried out over all X, Y, Z such that $F \equiv |X| + |Y| + |Z| \leq 10$. The contribution of anions at ten lattice parameters from the origin was less than 1% of the total energy computed. The profiles are reflected along the $m = 0.5$, $n = 0.5$, and $m = n - 1$ lines. The energy surfaces are not simple. There are local maxima, saddle points, and minima. The anions are surrounded by infinitely high potential walls. The cation will be at one of the minima. Physically, the reason that the cation at $l = 0$ lies along the perpendicular bisector of two anions rather than on the line joining the anions is that the short-range shell overlap repulsion energy predominates over the charge-induced dipole attraction energy. The relative strengths of these two can also be seen from the fact that even at $l = 0$ there is a local maximum at $m = n = 0.5$ due to the body centered anion at $l = 0.5$. As l increases, the energy at the four corners drops from $+\infty$ and that of the local maximum at the center increases until at $l = 0.25$ (Figure 4) there are equivalent maxima at all five points. This is as expected, since the corner and the center anions are equidistant from this plane. The energy profiles of $l = 0$ and $l = 0.5$ (Figure 5) are related, as we expect them to be. Since the position of the anions has been shifted by half a lattice parameter in each direction, we expect the energy profile will be so shifted too; that is, $E(c_1; 0, m, n) = E(c_1; 0.5, m + 0.5, n + 0.5)$. Not surprisingly, the potential walls are now around $m = n = 0.5$ where the anion is found, and there are local maxima at the four corners. The energy profiles for values of l greater than 0.5 are identical to those for that value of l reflected through $l = 0.5$; that is, for $l > 0.5$ and for all m and n, $E(c_1; l, m, n) = E[c_1; 0.5 - (l - 0.5), m, n]$.

The profiles have been presented here not only because they are interesting in their own right, but because they demonstrate the difficulties to be expected in obtaining the activation energy ΔE for a given lattice. The usual indirect method would be to solve Equations (7) numerically subject to inequalities (8) to obtain the minimum position (m^*, n^*) for each value of l. The values obtained would be used to solve Equation (10) subject to inequalities (11). However between $l = 0.25$ and $l = 0.5$, note that the saddle points, which are also solutions of Equations (7), are very close to the minima.

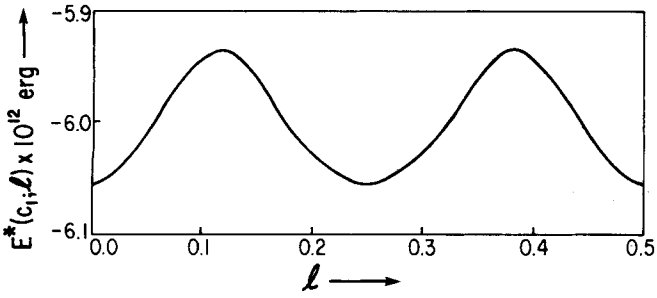

Fig. 6. Energy path of Ag^+ in α-AgI from $l = 0$ to $l = 0.5$. The path from $l = 0.5$ to $l = 1$ is a mirror image. The parameters are those of Figures 3 to 5.

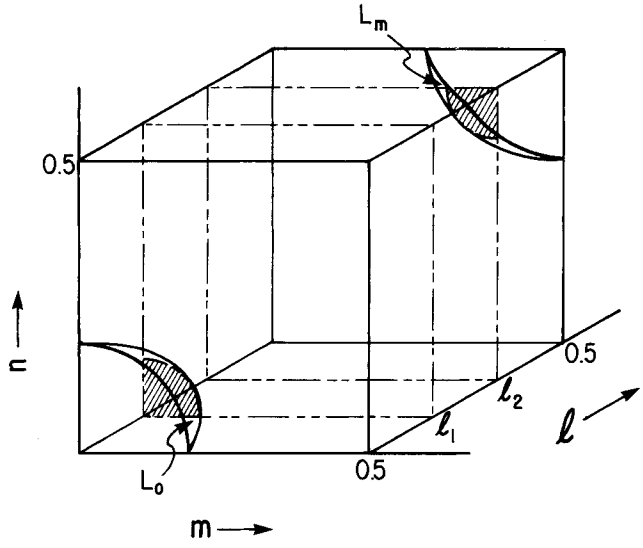

Fig. 7. To demonstrate the form of excluded zones at l_1, l_2. L_0 and L_m are the locii of artificial maxima surrounding corner and center anions, respectively, that is, the surfaces of the excluded zones.

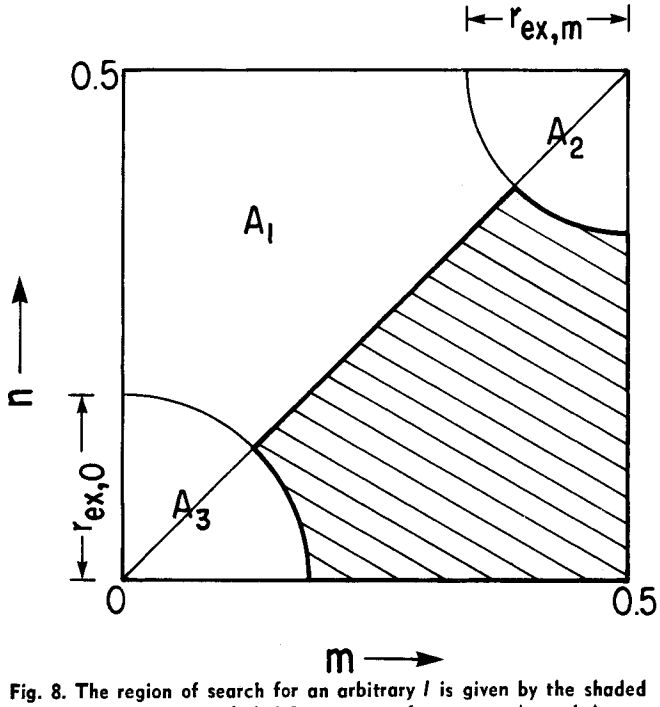

Fig. 8. The region of search for an arbitrary l is given by the shaded area. Area A_1 is not included for reasons of symmetry A_2 and A_3 are the excluded areas corresponding to the spheres of surfaces L_o, L_m in Figure 7.

It would require a very elaborate scheme of computation to avoid the saddle points, which are not of interest, and approach only the minima. Conventional direct computation techniques such as the complex method (Box, 1965), which can distinguish saddle points from minima, are too slow to converge; besides, there is usually more than one minimum. Since m and n are very limited in range, a search procedure can be used. This evaluates Equation (13) for a series of values of m and n in the range $[0, 1)$, keeping only the minimum value $E^*(c_1;l)$ for each l. The largest and the smallest values of $E^*(c_1; l)$ for a given c_1 are then substituted in Equation (9) to obtain the activation energy $\Delta E(c_1)$. Since we are not interested in the absolute energy values, it is reasonable to assume that any errors will be removed in the subtraction of Equation (9). The energy path for a silver ion in the α-silver iodide lattice is presented in Figure 6. The path was reflected at $l = 0.5$. The activation energy ΔE could be deduced from the figure.

NUMERICAL COMPUTATION OF THE ACTIVATION ENERGY

For various values of c_1 and the corresponding values of r_j and α_j, the energy path of the silver ion was obtained and the activation energy calculated by the search procedure outlined in the previous section. Since the energy profiles were found earlier to be eightfold symmetric in m and n, the region of interest for any l could be greatly reduced with no adverse effects. In this work it was taken to be the area bounded by and including the lines $m = 0.5$, $n = 0$, and $m = n$. However, another exclusion in this area was necessary. As mentioned earlier, the cation could not occupy any part of the lattice volume bounded by the artificial maxima a reduced distance r_{ex} from the center of the stationary anions. In general, the (m, n) plane at an arbitrary value of l would have an excluded zone of a quadrant centered at (0, 0) with radius $r_{ex,0}$, as in the plane at l_1 in Figure 7, and another excluded quadrant with center (0.5, 0.5) and radius $r_{ex,m}$, as in the plane at l_2. The excluded regions are shown in Figure 8. The quadrants are formed from spheres of (reduced) radius r_{ex} and centers at $l = 0$, $m = 0$, $n = 0$, and $l = 0.5$, $m = 0.5$, $n = 0.5$ corresponding to the corner and center anions respectively. The radii of the quadrants are related to l and r_{ex} by

$$r_{ex,0}(l) = \begin{cases} (r_{ex}^2 - l^2)^{1/2} & l < r_{ex} \quad (16a) \\ 0 & l \geq r_{ex} \quad (16b) \end{cases}$$

$$r_{ex,m}(l) = \begin{cases} 0 & l \leq 0.5 - r_{ex} \quad (17a) \\ [r_{ex}^2 - (0.5 - l)^2]^{1/2} & l > 0.5 - r_{ex} \quad (17b) \end{cases}$$

The value of r_{ex} for each anionic lattice was obtained numerically as the smallest nonzero value of n for which $E(c_1; 0, 0, n)$ was a maximum.

It was found that anions from $F = 5$ lattice distances to $F = 10$ lattice distances added terms to the total interaction energy $E^*(c_1; l)$ that were practically independent of l. Hence, they contributed nothing to the value of $\Delta E(c_1)$ as given in Equation (9) and could be easily omitted from the calculation of $E(c_1; l, m, n)$ in Equation (13) with a very significant saving in computation time.

RESULTS AND DISCUSSION

Figures 9 and 10 illustrate the energy paths of a silver anion in the sulfide and the selenide lattices respectively. The activation energies ΔE are plotted in Fig-

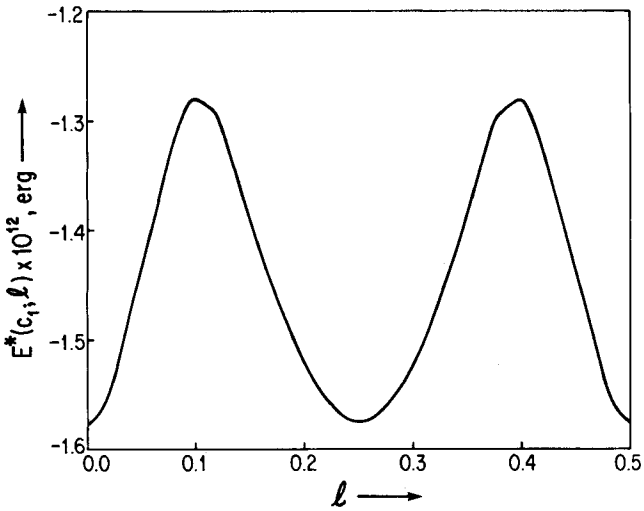

Fig. 9. Energy path of Ag^+ in the α-Ag_2S lattice. The parameters are those of Table 1.

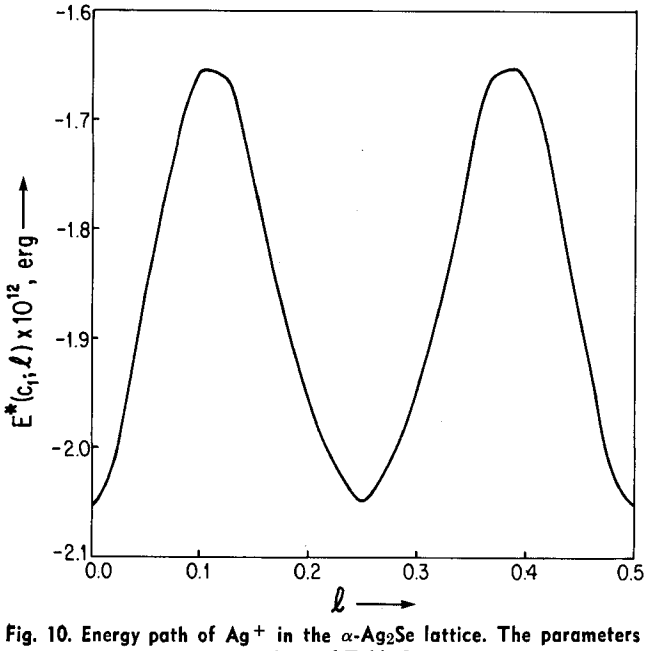

Fig. 10. Energy path of Ag^+ in the α-Ag_2Se lattice. The parameters are those of Table 1.

ure 11 as a function of the lattice parameter c_1. The parameters r_j and α_j were obtained by the interpolation relations (15). The monotonic increase in activation energy as c_1 increases is due to the fact that the minimum of the energy path at $l = 0$, 0.25 and 0.5 drops faster than the maximum at $l \sim 0.1$ and 0.4.

The energy path for the mono-monovalent silver iodide using the parameters of Table I is shown in Figure 12. It is unusual in that minimum interaction energies $E^*(c_1; l)$ are positive (repulsive) over a significant fraction of the path. This illustrates the effect of crowding of the anionic lattice, in that the cation is not able to move far enough away from an anion to be in its attraction field before the cation encounters the repulsion field of a neighboring anion.

Using Equations (14) in Equations (13) and the value of c_f, etc. from Table I, the activation energy for the transport of the silver ion in the fcc telluride lattice is

$$\Delta E = 11.7 \times 10^{-13} \text{ erg/ion} \qquad (18)$$

Even though the lattice parameter c_f of α-Ag_2Te is larger than the c_1's of α-Ag_2Se or α-Ag_2S, the telluride lattice is

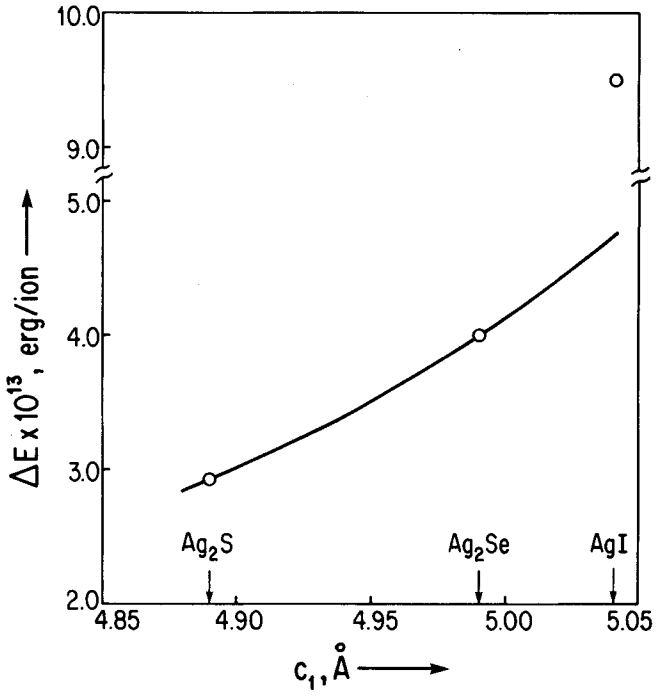

Fig. 11. Activation energy as a function of lattice parameter. Open circles show positions of the lattices of the pure compounds α-Ag_2S, α-Ag_2Se, and α-AgI. Properties of the other lattices are obtained by interpolation and extrapolation of the first two [Equations (15)].

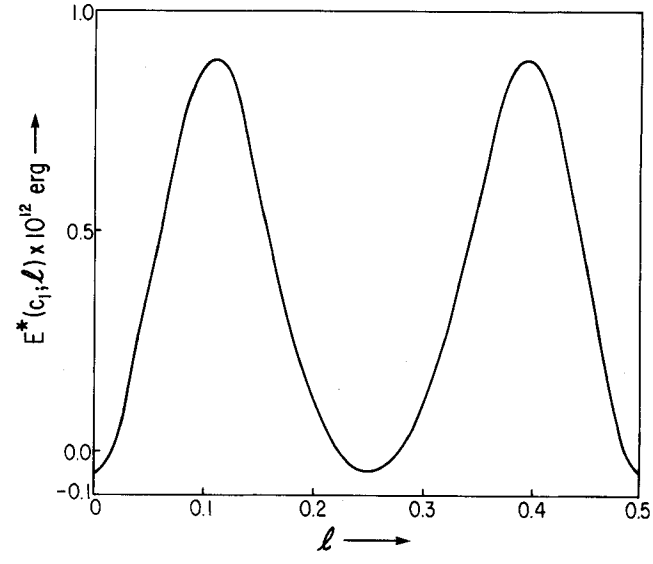

Fig. 12. Energy path of Ag^+ in α-AgI. Parameters are those of Table 1.

more crowded than the other two since the telluride ionic radius is larger than those of the sulfide and selenide and there are in the fcc unit cell a larger number of anions than in the bcc unit cell. This relative crowding probably causes the larger value of ΔE in Equation (18), as compared to those of Figure 11. To illustrate this point, the calculations were repeated for a "corresponding" bcc lattice, i.e. one that had the same nearest neighbor distance as that of the fcc lattice. For $c_f = 6.59$Å, the nearest neighbor distance is 4.65Å; the bcc lattice with the same nearest neighbor distance has the parameter $c_1 = 5.37$Å. Using this value in Equation (6) the corresponding activation energy is

$$\Delta E = 5.28 \times 10^{-13} \text{ erg/ion} \qquad (19)$$

This is less than that of (18), as expected.

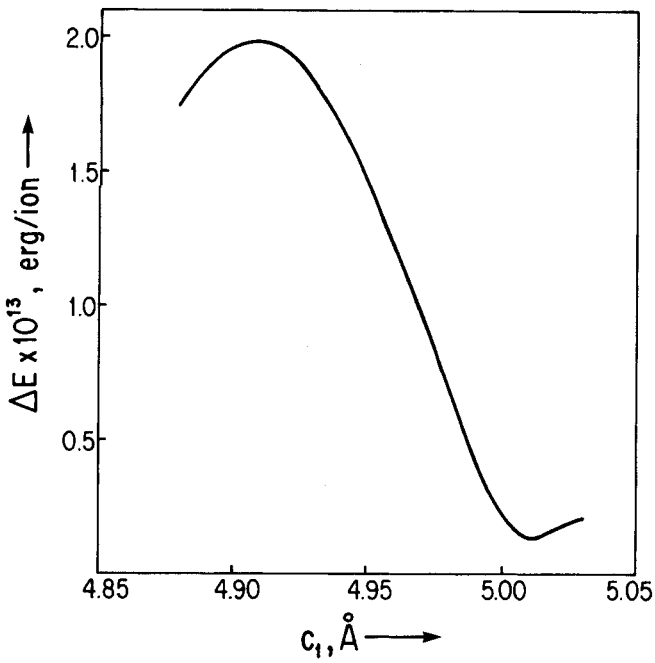

Fig. 13. Activation energies of the hypothetical di-divalent lattices of the α-type.

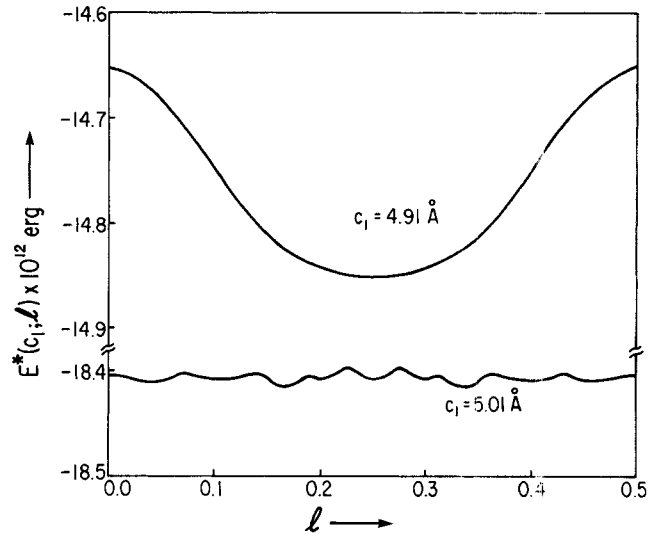

Fig. 14. Energy paths of ion in lattices corresponding to the maximum (top) and minimum (bottom) activation energies of Fig. 13. Parameters from Equation (15) and Table 1.

Now consider a set of hypothetical lattices, also of the α-form, but different from those of Figure 11 in that the mobile cation is also divalent, that is, $z_i = 2$. (This perhaps corresponds to Cd^{+2}.) It must be emphasized, however, that such a structure, to the best of our knowledge, has no physical reality and is presented here only for illustrative purposes. The activation energies in this case are plotted in Figure 13. The existence of extrema here may be noted.

In Figure 14, we show the energy paths that provide maximum and minimum activation energies in the hypothetical lattices of Figure 13. There is a distinct difference between the two. The upper curve has one deep minimum at $l = 0.25$ (and $l = 0.75$) and maxima at $l = 0$ and $l = 0.5$ (and at $l = 1$) so that ion transport could be considered as an activated process. On the other hand the lower curve gives rise to a large number of oscillations in the energy path of the cation with an almost nonexistent distinction between local and absolute minima, i.e. almost channel flow.

COMPARISON WITH OBSERVED VALUES

Table 2 shows the values of our calculated activation energy of interaction compared with activation energies obtained from the temperature dependences of conductivity and diffusion coefficients as collected by Wiedersich and Geller (1970) and Friauf (1972). The value computed for the α-silver sulfide is in good agreement with experiment. For α-silver iodide, the calculated value was significantly improved when the parameters of Figure 3 were used. The small increase in activation energy from the sulfide to the selenide was not observed experimentally. It is curious that the value of activation energy from conduction experiments on the α-silver telluride is so much greater than that from diffusion experiments; the increase is probably due to the polycrystallinity of the sample used for the conduction experiments. The calculated activation energy for this compound is somewhat higher than that for conduction.

The calculated values of ΔE depended upon various parameters. Most of these are well formulated: the polar-

TABLE 2. COMPARISON WITH EXPERIMENTS

Compound	Theoretical value	Observed values				
		Diffusion*			Conductivity†	
	ΔE†† eV	Temp. range, °C	h_σ,†† eV	h_T,†† eV	Temp. range, °C	W,†† eV
α-AgI	0.60	146-555	0.10	0.14	220-530	0.051
	0.08**				145-555	0.064
α-Ag_2S	0.18	177-831	0.11	0.14	180-300	0.11
α-Ag_2Se	0.24	133-880	0.10	0.12	130-300	0.10
α-Ag_2Te	0.70	145-802	0.14	—	165-225	0.31

* Data collected by Wiedersich and Geller (1970).

** ΔE value for anionic radius r_j = 1.75 Å; polarizability α_j = 6.024 Å^3.

† Data collected by Friauf (1972). Polycrystalline samples were used.

†† ΔE: activation energy of interaction

h_σ, h_T: activation enthalpy obtained from conductivity and Ag^+-tracer diffusion.

W: activation energy from conductivity.

izability α_j, the cell length c_1, and others. The anionic radius r_j has not been uniquely characterized, various authors having obtained differing values for the same anion (see, for example, Shannon and Prewitt, 1969). It is conceivable, therefore, that the varying values of observed activation energies can be traced to different effective ionic radii for diffusion and for conduction.

ACKNOWLEDGMENT

We are indebted to Dr. Leah Gal-Or for stimulating discussions concerning solid electrolytes.

NOTATION

A = monopole-induced dipole attraction constant, Equation (5)

A_1, A_2, A_3 = areas not included in the region of search, Figure 8

B = overall repulsion constant, Equation (5)

b = repulsion constant, Equation (3)

C = Coulomb interaction constant, Equation (5)

c_1, c_2, c_3 = lattice distance parameters

$\mathbf{c}$ = lattice distance vector (c_1, c_2, c_3)

c_{+-} = overlap constant, Equation (3*b*)

c_f = fcc lattice distance parameter

$E(\mathbf{c}; l, m, n)$ = interaction energy between a mobile ion and a lattice, Equation (5)

$E(c_1; l, m, n)$ = interaction energy between a cation and an array of anions, Equation (13)

$E^*(c_1; l)$ = minimum interaction energy at a given l

e = charge of an electron

f_{1j}, f_{2j}, f_{3j} = reduced position of j^{-th} lattice ion

F = spacing between anion and cation, $= |X| + |Y| + |Z|$

h_σ, h_T = activation enthalpy observed from conduction, diffusion experiments

J = number of ions per unit cell, Equation (5)

L = position of local maximum in energy profiles, Figures 3 to 5

L_o, L_m = locii of artificial maximum (surface of excluded zone), Figure 7

l = reduced position coordinate of cation

l_{max} = value of l for which energy path is at its highest peak

l_{min} = value of l for which energy path is at its lowest valley

M = position of anion in energy profiles, Figures 3 to 5

m = reduced position coordinate of cation

m^* = value of m corresponding to minimum of cation energy profile at a given l

N = position of minimum in energy profiles, Figures 3 to 5

N_i, N_j = number of electrons in outermost (closed) shell of cation, anion

n = reduced position coordinate of cation

n^* = value of n corresponding to minimum of cation energy profile at a given l

r_{ex} = distance between center of anion in array and artificial maximum corresponding to anion; radius of excluded sphere

$r_{ex,0}, r_{ex,m}$ = radii of excluded quadrants, Figure 8

r_i, r_j = ionic radii

r_{ij} = distance between mobile and lattice ions

r_{i1}, r_{i2} = distance between mobile cation and corner, center anions of bcc or bct lattice

r_{max}, r_{min} = interionic distances corresponding to maximum and minimum of pair interaction energy, Figure 1

S = position of saddlepoint in energy profiles, Figures 3 to 5

X, Y, Z = number of unit cells separating cation and anion in the three dimensions

z = ionic charge integer

Greek Letters

α = polarizability

ρ = repulsion parameter

∂ = partial differential operator

Δ = change, ΔE, activation energy

σ = conductivity

Subscripts

c = Coulomb

d = dipole

i = cation, mobile ion

j = anion, lattice ion

s = shell overlap

LITERATURE CITED

Batist, Ph. A., A. H. W. M. der Kinderen, Yvonne Leeuwenburgh, Francien A. M. G. Metz, and G. C. A. Schuit, "The Catalytic Oxidation of 1-Butene over Bismuth Molydate Catalysts. IV. Dependence of Activity on the Structures of the Catalysts," *J. Catal.*, **12**, 45 (1968).

Box, M. J., "A New Method of Constrained Optimization and a Comparison with Other Methods," *Computer J.*, **8**, 42 (1965).

Cubiccioti, D., "Lattice Energies of the Alkali Halides and the Electron Affinities of the Halogens," *J. Chem. Phys.*, **31**, 1646 (1959).

Donnay, J. D. H., ed., *Crystal Data Determinative Tables*, 2 ed., ACA Monograph No. 5, American Crystallographic Association (1963).

Friauf, R. J., "Tables of Ionic Conductivity and Diffusion in Ionic Crystals," in *Physics of Electrolytes*, Vol. 2, J. Hladik, ed., pp. 112 et seq., Academic Press, New York (1972).

Flygare, W. H., and R. A. Huggins, "Theory of Ionic Transport in Crystallographic Tunnels," *J. Phys. Chem. Solids*, **34**, 1199 (1973).

Geller, S., "Crystal Structure of the Solid Electrolyte (C_5H_5NH) Ag_5I_6 at $-30°C$," *Nature*, **176**, 1016 (1972).

———, and M. D. Lind, "Crystal Structure of the Solid Electrolyte $[(CH_3)_4N]_2$ $Ag_{13}I_{15}$," *J. Chem. Phys.*, **52**, 5854 (1970).

Hirschfelder, J. O., C. F. Curtiss, and R. B. Bird, *Molecular Theory of Gases and Liquids*, Sect. 12.1, 12.2, Wiley, New York (1954).

Hoshino, S., "Crystal Structure and Phase Transition of Some Metallic Halides III. Structure Anomaly in α-Ag_2HgI_4," *J. Phys. Soc. Japan*, **10**, 197 (1955).

Pauling, L., "The Sizes of Ions and their Influence on the Properties of Salt-like Compounds," *Z. Krist.*, **67**, 377 (1928).

Rahlfs, P., "On the Cubic High Temperature Modifications of the Sulfide, Selenide and Telluride of Silver and Monovalent Copper," *Z. Phys. Chem.*, **B 31**, 157 (1936).

Rice, O. K., *Electronic Structure and Chemical Bonding*, pp. 171 et seq., McGraw Hill, New York (1940).

Rich, R., *Periodic Correlations*, pp. 60-61, W. A. Benjamin, Inc., New York (1965).

Shannon, R. D., and C. T. Prewitt, "Effective Ionic Radii in Oxides and Fluorides," *Acta. Cryst.*, **B25**, 925 (1969).

Strock, L., "Crystal Structure of High Temperature Silver Iodide, αAgI," *Z. Phys. Chem.*, **B25**, 441 (1934).
van Gool, W., "Fast Ion Conduction," in *Annual Review of Material Science*, Vol. 4, R. A. Huggins, ed., p. 311 et seq., Annual Reviews, Inc., Palo Alto, Calif. (1974).
Wiedersich, H., and S. Geller, "Properties of Highly Conducting Halide and Chalcogenide Solid Electrolytes," in *The Chemistry of Extended Defects in Non-Metallic Solids*, L. Eyring and M. O'Keefe, ed., p. 646 et seq., North Holland, Amsterdam (1970).

Manuscript received January 5, 1976; revision received and accepted March 22, 1976.

The Hydrodynamic Resolution of Optical Isomers

A potentially simple and effective technique is proposed for separating enantiomorphic crystal pairs from each other, or separating individual enantiomorphs from optically active impurities.

This method consists essentially of settling under conditions controlling orientation of the asymmetric particles and taking advantage of the tensorial nature of their friction factors.

D. W. HOWARD
E. N. LIGHTFOOT
and
J. O. HIRSCHFELDER
The University of Wisconsin
Madison, Wisconsin 53706

SCOPE

A new and potentially simple method is proposed for resolving racemic mixtures of optically active substances. Separation is achieved purely by hydrodynamic means, without conversion of the components to geometric isomers. The procedure suggested is essentially a means for automating the mechanical sorting technique of Pasteur for separation of enantiomorphic crystals.

CONCLUSIONS AND SIGNIFICANCE

Experiments with a variety of crystals and crystal models demonstrate the effectiveness of hydrodynamic forces for producing such separations. It remains, however, to refine the orientation techniques and to establish effective crystallization procedures

Where the proposed method is feasible, it should substantially facilitate both the resolution of enantiomorphs and the separation of optically active crystals from inactive solids. It is particularly promising for reducing the costs of pharmaceuticals and food or feed additives as an alternate to present resolution procedures.

Resolving racemic mixtures of optically active compounds is important in the synthesis of food or feed additives and pharmaceuticals, and it can be both tedious and expensive. In addition, presently used procedures, all of which involve chemical reactions with one isomer of a second optically active species, are quite complex in comparison with Pasteur's classic mechanical resolutions of tartrate salts (Pasteur, 1847, 1850). His procedure was simply to crystallize a racemic mixture under conditions yielding pure crystals of the individual enantiomorphs and to separate these mechanically under a low-power microscope. His technique is expensive only because of the amount of labor required, and we decided to see if the sorting process could be automated. We proposed to do this by utilizing the peculiar hydrodynamic properties of enantiomorphic crystals, which typically have a pronounced screw sense, or skewness.

The impetus for this project was repeated reports that the right and left shells of bivalves sometimes turn up in significantly different numbers on ocean beaches (Lever, 1958, 1961, 1964; Nagle, 1964, 1967). Many of these shells closely approximate the mirror image asymmetry of enantiomorphic pairs, and they may be considered as crystal analogues. It therefore appeared that effective spontaneous resolution was being achieved in relatively simple flow situations.

We began by seeking suitably asymmetric conditions for the separation either of the optically active molecules themselves or their crystals, which generally show the same type of mirror image asymmetry. As a guide in this search, it was useful to review the transport behavior of skew particles at both the molecular and macroscopic levels.

THEORY

All optically active molecules lack a plane of symmetry, and the mirror image relation of enantiomorphic pairs suggests that, for any given molecular orientation, they will move in different directions when acted on by the same

D. W. Howard is with Savannah River Laboratories, E. I. duPont de Nemours & Company, Aiken, South Carolina.